Latitudinal beaming of Jupiter's radio emissions from Juno/Waves flux density measurements

https://doi.org/10.1029/2021JA029435

C. K. **Louis**[1,2,3], P. Zarka[1], K. Dabidin[1], P.-A. Lampson[1], F. P. Magalhães[1], A. Boudouma[1], M. S. Marques[4], and B. Cecconi[1]

corentin.louis@dias.ie

[1] LESIA, Observatoire de Paris, PSL, CNRS, Meudon, France ; [2] School of Cosmic Physics, DIAS Dunsink Observatory, Dublin, Ireland ; [3] Institut de Recherche en Astrophysique et Planétologie (IRAP), CNRS, CNES, University of Toulouse, France ; [4] Departamento de Geosica, Universidade Federal do Rio Grande do Norte, Brazil

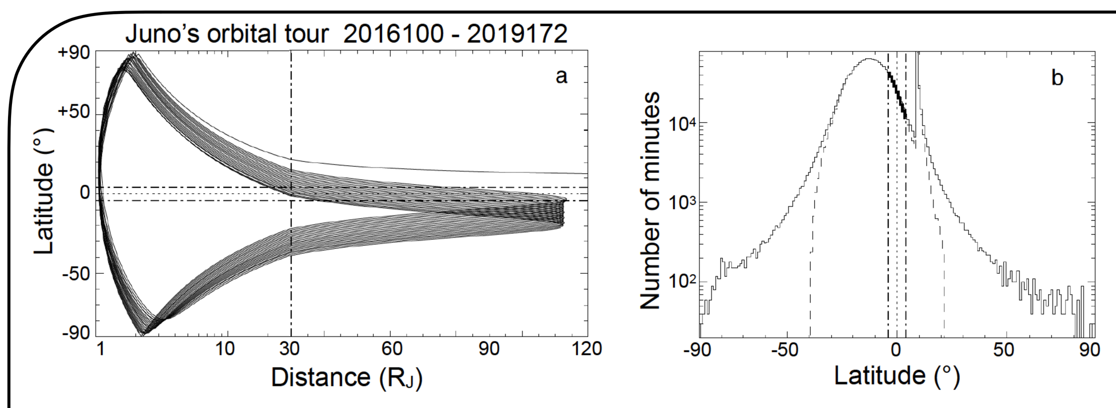

Figure 1. (a) Jovicentric latitudes explored by Juno as a function of the distance between DoY 100 of 2016 (2016/04/09) and DoY 172 of 2019 (2019/06/21). The distance scale is logarithmic between 1 and 30. The processing pipeline is based on data recorded at latitudes within ±4° of the equator (magnetic latitude within ±14°) and beyond 30 RJ (dash-dotted lines). (b) Time (in minutes) spent by Juno within each 1° bin of latitude during this 3-year interval (solid line). The dashed line is the time spent by Juno at distances ≥30 RJ . The thick line, within ±4° of latitude, corresponds to the data used in our processing pipeline (the peak around +10° corresponds to Juno's approach trajectory).processing pipeline (the peak around +10° corresponds to Juno's approach trajectory).

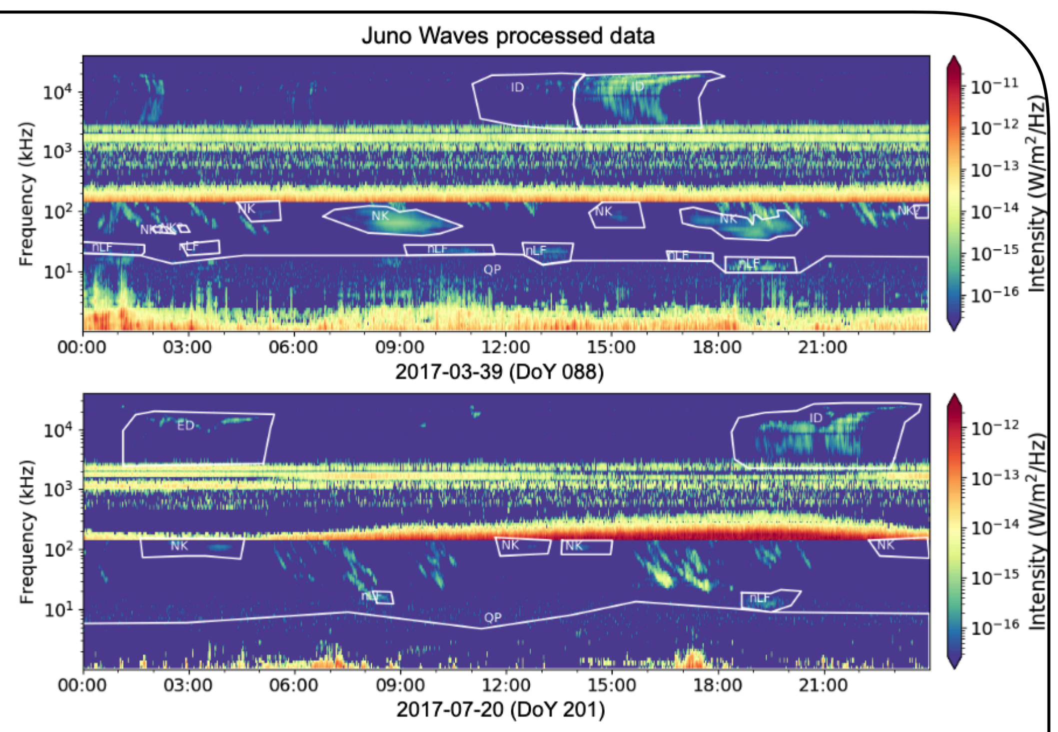

Figure 2. Example of two 24-hour dynamic spectra of processed Juno/Waves data (DoY 88 and 201 of 2017). Catalogued events are indicated by the white contours and labels. The ubiquitous drifting features below 150 kHz are bKOM, emission patches and arcs not otherwise identified above 3 MHz are auroral HOM and DAM emissions.

Radio component	Minimum - Maximum frequency
QP	1 - 140 (900) kHz
nLF	1.3 - 130 kHz
nKOM	12 - 140 (250) kHz
bKOM	1 - 140 (800) kHz
HOM & DAM (auroral)	(0.14) 3.5 - 41 MHz
Io-DAM	(0.14) 3.5 - 40 MHz

Table: Frequency ranges covered by each component. The limits in parentheses fall into the HFR-low band and thus only concern the few events detected near the perijoves. For our statistical study, we exclude the HFR-low band thus the frequency ranges used are those not in parentheses.

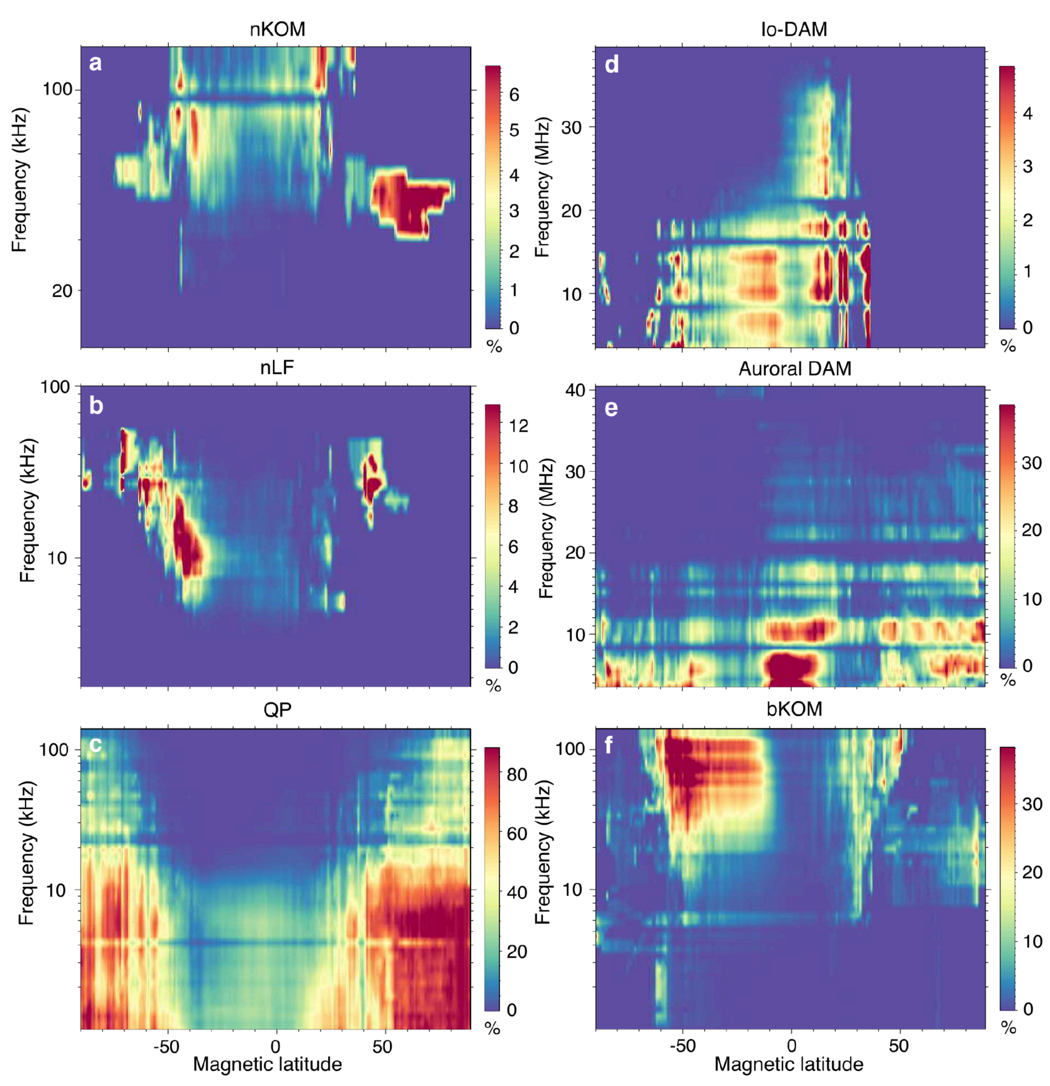

Figure 3. Occurrence probability of each Jovian radio component as a function of Juno's magnetic latitude and frequency. Latitude bins are 1° wide and frequencies are those of Juno/Waves channels.

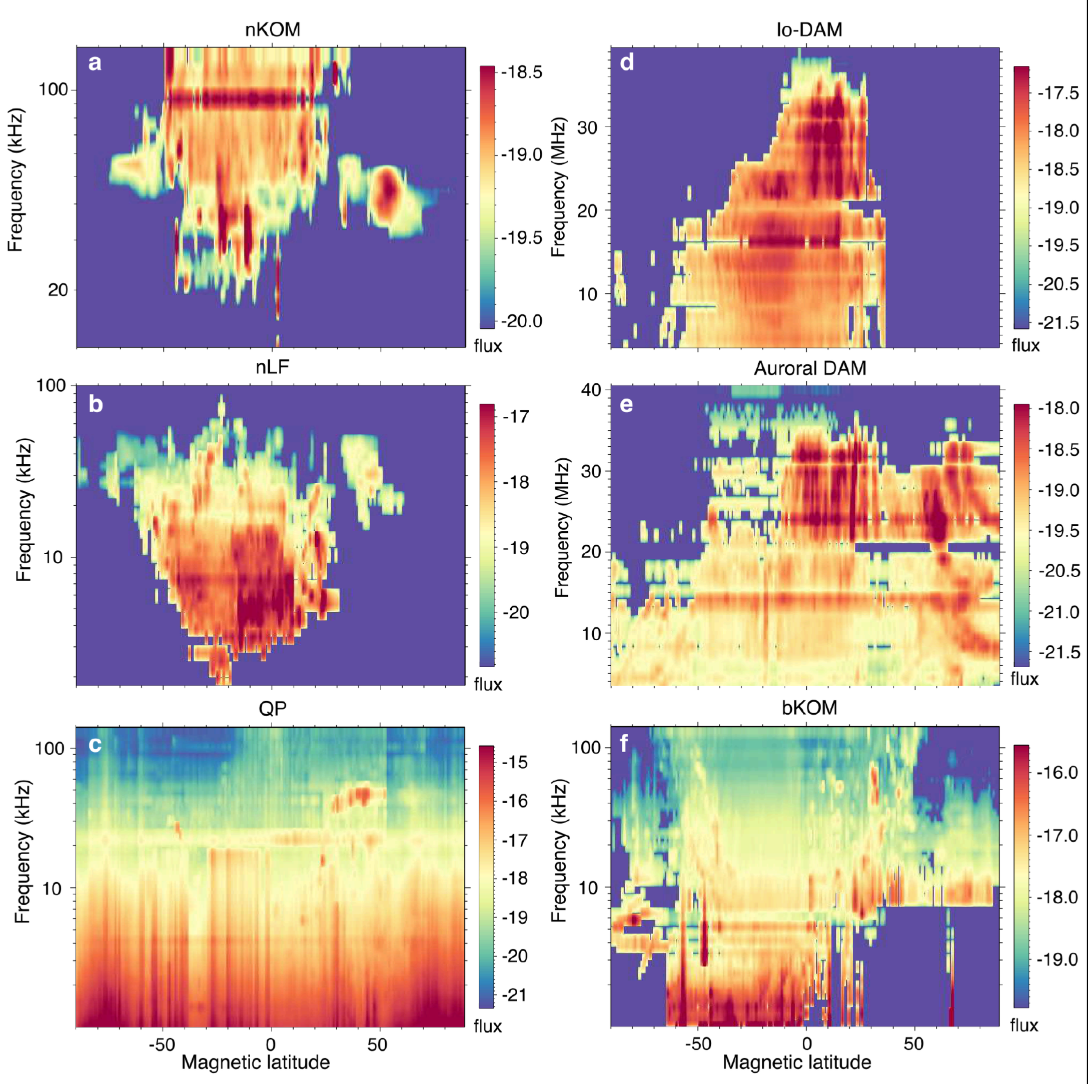

Figure 4. Intensity normalized to a distance of 1 AU (in W/m2/Hz) of each Jovian radio component as a function of Juno's magnetic latitude and frequency. Latitude bins are 1° wide and frequencies are those of Juno/Waves channels.

Appendix : Flux density estimation of Juno/Waves

Pre-processing of Juno/Waves data

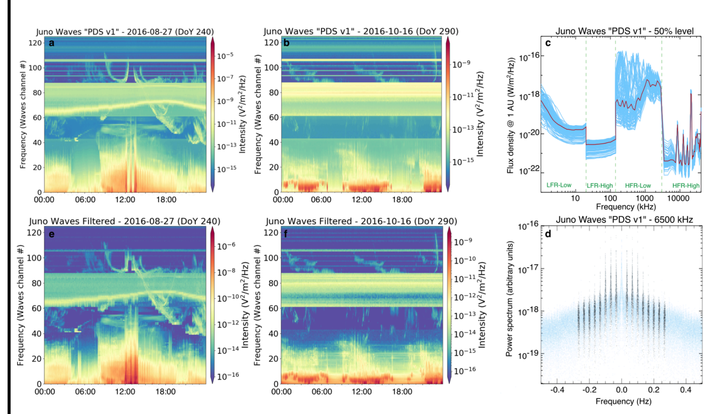

Figure A1. (a) Dynamic spectra of 24 h of Juno/Waves "PDS v1" survey data around perijove 1. Y-axis is in channel number, that combines log-spaced frequencies <3 MHz (channel #87) and linearly-spaced frequencies above that frequency. Intensities are in $V^2/m^2/Hz$. Ephemeris information is listed along the X-axis. (b) Same as (a) for 24 h between perijoves 1 and 2, at 40 to 50 R_J from the planet. (c) Median flux density spectra derived from Juno/Waves PDS-v1 data over 120 selected intervals (in blue) and their overall median spectrum (in red), normalized to an observer's distance of 1 AU. Intensities have been converted to $W/m^2/Hz$ by a simple division by the impedance of free space (Z_0=377 Ω). (d) Power spectrum of a time series of Juno/Waves measurements in channel 91 (6.5 MHz). Blue parts of the power spectrum are set to 0 for filtering out interference not modulated by the spacecraft rotation and its harmonics (these are the intervals $N/30 \pm 0.005$ Hz, with $N = 1, 8$, displayed in black). (e,f) Same as (a,b) after FFT-filtering (d).

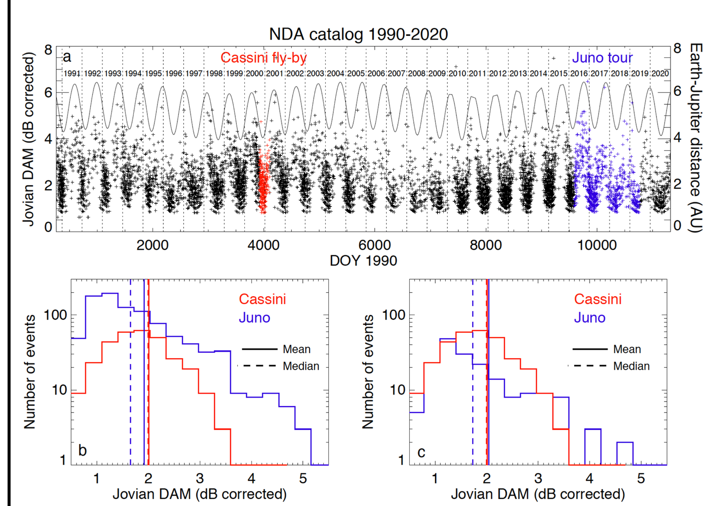

Figure A2. (a) DAM intensity from the Nançay Decameter Array catalog 1990-2020 (extended from Marques et al., 2017), averaged on each event of the catalog (of duration between a few minutes and 5 hours). Intensity values have been corrected for the variable Earth-Jupiter distance, also displayed in the figure. Measurements during the Cassini flyby are displayed in red, and those during the Juno tour (for the 3-year interval studied) in blue. (b) Histograms of DAM intensities measured with the NDA during the Cassini and Juno eras, with indication of the mean (solid line) and median (dashed line) of each histogram. (c) Same as (b) with the Juno era histogram computed only over the 120 intervals selected for our processing.

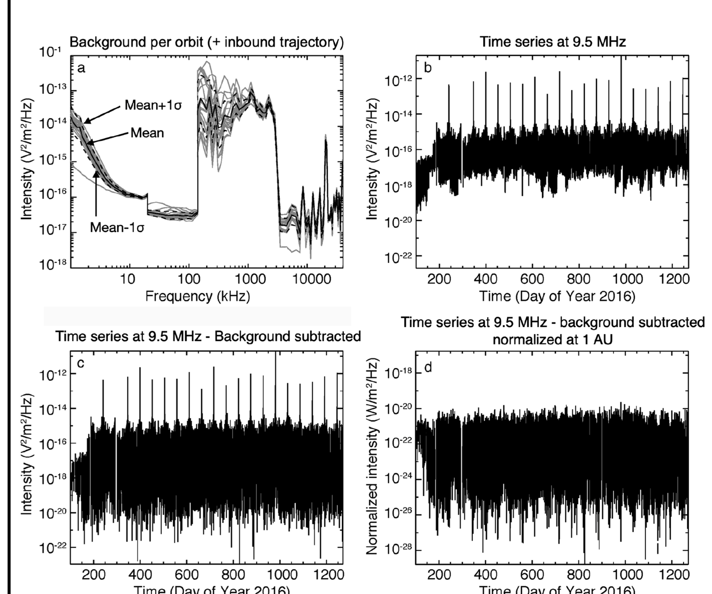

Figure A3. (a) Background spectra of Juno/Waves FFT-filtered survey measurements per Juno's orbit (+ during the inbound trajectory from 2016/04/09 to perijove 0 on 2016/07/05) are displayed in grey. The background with a lower low-frequency part is the one corresponding to the inbound trajectory, over which no Jovian trapped continuum is detected. The mean background is the black solid line, with its 1σ variations limited by the dashed lines. (b) Time series of FFT-filtered intensities in channel 94. (c) Same as (b), after subtraction of mean background from (a). (d) Same as (c) after normalization to an observer's distance of 1 AU and conversion to flux densities.

Converting pre-processed data → flux densities

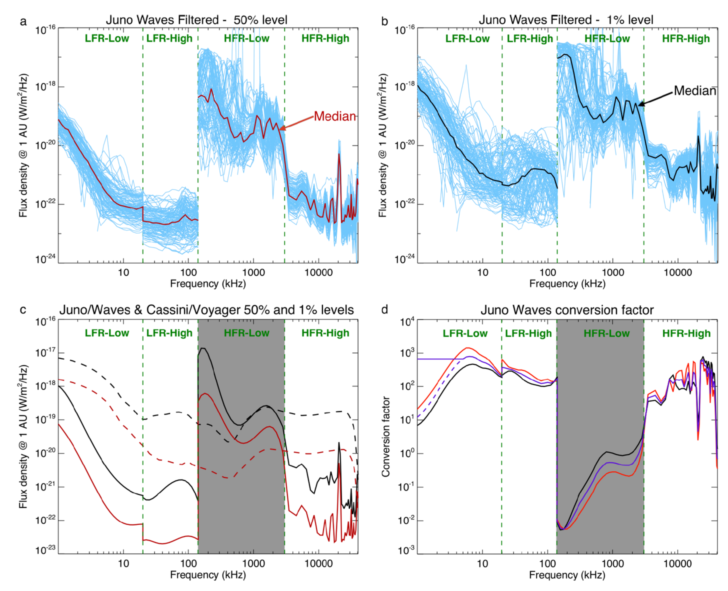

Figure A4. (a) Median flux density spectra computed over the 120 selected intervals of Juno/Waves data, after FFT-filtering, background subtraction and normalization to an observer's distance of 1 AU (blue lines). The red line is the median over all individual median spectra. (b) same as (a), but for the first percentile spectra i.e. the flux density at each frequency exceeded by 1% of the measurements in each of the 120 intervals. The black line is the median over all individual 1% occurrence spectra. (c) Smoothed median spectra from panels (a) and (b) (solid lines) and Cassini-Voyager 50% and 1% spectra derived as explained in the caption of Figure S1 (dashed lines). The HFR-low band is grey-shaded because this procedure based on long-term statistics does not apply to it (see text). (d) Conversion curves deduced from the ratios of Cassini-Voyager to Juno 50% (red) and 1% (black) spectra from panel (c). The purple line is the geometrical average of the red and black curves. A constant value is used below 5 kHz in replacement of the computed ones (dashed), to take into account the presence of trapped continuum

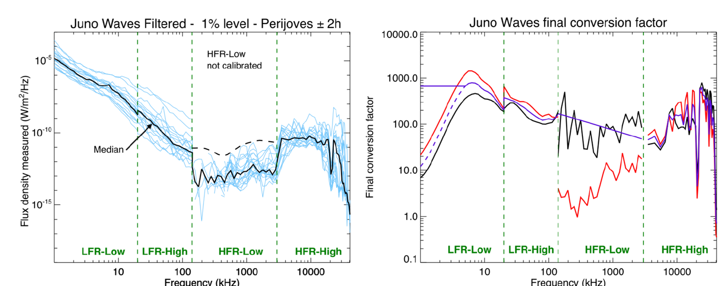

Figure A5. Same as Figure A4 but focused on the perijoves, for estimating the flux density of the HFR-low band.(a) First percentile spectra i.e. the flux density at each frequency exceeded by 1% of the measurements in each of the 19 intervals around perijoves. The black line is the median over all individual 1% occurrence spectra. Measurements have been processed and converted to flux densities in LFR-low, LFR-high and HFR-high bands, and pre-processed only (FFT-filtered, background subtracted) in the HFR-low band. The dashed curve is the portion of the Cassini 1% reference spectrum (from Figure A4c), up-scaled to match the level of the signals on both sides of the HFR-low band. (b) Same as Figure A4d, completed by the conversion curve in the HFR-low band. The black line is deduced from panel (a). The red line is deduced from 50% spectra, which are too much polluted to be used for our processing procedure. The purple line is the linear interpolation of the black line that matches the conversion curve at both edges of the HFR-low band.

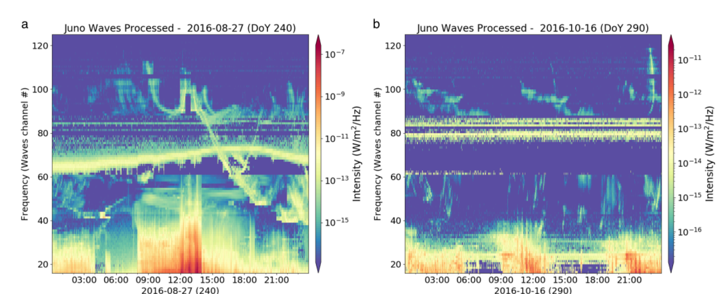

Figure A6. Processed versions derived from Figures A1a,b and then A1e,f by application of the conversion curve of Figure A5b.

Main conclusions

(1) All low-frequency components (nLF, nKOM, bKOM, QP) display minimum occurrence near the equator, maxima at mid-latitudes, except QP bursts (max ~ ±90°)

(2) All radio components except HOM have a highly asymmetric occurrence in latitude; nLF, nKOM, bKOM and QP have their overall lat.-freq. pattern shifted to the South; minimum occurrence of bKOM is centered ~ +10° latitude, with asymmetric gradients on both sides

(3) nLF and bKOM show higher occurrences in the South

(4) QP bursts have a higher occurrence in the North, with a larger extent towards lower latitudes in the North; low occurrence at low latitudes, increases toward higher freq. at high lat. (QP bursts ~ uniformly intense at all latitudes)

(5) bKOM occurrence has high-latitude extents at 10-60 kHz

(6) nLF and nKOM occurrences have high latitude extents (up to ±80°) at resp. 20-50 kHz and 30-60 kHz; similar morphologies, very ≠ from that of bKOM => unique component?

(7) Occurrence of nLF and nKOM ~0 at the highest N and S latitudes (this is also the case for Io-DAM but we rather attribute it to a selection effect)

(8) Auroral DAM and Io-DAM reach higher frequencies in the North than in the South; high-frequency emission absent below < -5° to -10° suggesting that N emission is not detected from the S hemisphere (and vice-versa?)

(9) Order of decreasing occurrence: QP bursts, bKOM, HOM, auroral DAM and nLF, and finally nKOM and Io-DAM

(10) Auroral HOM and DAM, Io-DAM, and QP components better organized in magnetic latitude; nLF and bKOM better organized in centrifugal lat.; unclear for nKOM

Tentative interpretations

(1) ≠ meaning for ≠ LF Jovian radio components; nKOM & nLF +**(10)** => emission produced at ~f_{pe} or f_{UH}(Io torus, plasmasphere, plasma sheet boundaries) → **See Poster of Boudouma et al.**

(1,7) peak mid-latitude occ. of nKOM and nLF → emission beamed // grad(Ne)? (nLF frequent in Juno data while rarely observed from near-equator) → **See Poster of Boudouma et al.**

(1) refraction on bKOM (auroral!) on the equatorial plasma → ray-tracing studies; consistent with **(10)** bKOM better organized in centrifugal latitude (although sources organized along B lines)

(1,4) QP bursts beamed towards high latitudes by propagation effects from high latitude sources ?

(9) QP occurrence extremely high (> 80%) at high latitudes, & better organized in mag. latitude → active auroral-related process

(2,3) N/S asymmetry related to asymmetric Jovian B field (& plasma), but no simple explanation available

(8,10) asymmetry of auroral & Io-DAM freq. ranges → CMI emission ~f_{ce} & Jovian B field stronger in the North; larger N occurrence less easy to explain

(8) emission observability ≠ ExPRES predictions → oblate emission cone model of Galopeau (2016) (cone opening < (B,∇B) plane than perpendicular to it)

(9) HOM occurrence (≤ 6-8 MHz) > auroral-DAM, especially S, & HOM emissions less intense → relationship HOM/DAM ?

(9) Io-DAM occurrence lowest but = potentially visible emissions (arc duration / Io's orbital period = 1-5% = observed) → Io-DAM ~ permanent

Future studies based on the catalog and absolute flux densities

- *Occurrence and intensity variations vs CML and frequency (Imai et al. 2011, K2 => extend to Juno data up to 40 MHz)*
- *Occurrence and intensity variations vs observer's LT => dawn/dusk asymmetry ? // UV ?*
- *Separate studies per Jovian radio component, compare statistical properties (3 to 9 years → statistical basis x3): long-term SW effects, variations of solar EUV flux, seasonal variations ?*
  → understand origin, beaming and relations between components

Data Availability: PDS v1 @ https://doi.org/10.17189/1519710 ; Processed data + conversion tables @ https://doi.org/10.25935/6jg4-mk86 ; ExPRES simulations @ https://doi.org/10.25935/kpge-zb59 ; Juno/Waves catalog @ https://doi.org/10.25935/nhb2-wy29

Acknowledgments: W. Kurth and the Juno/Waves team, CNES, PNST, PNP, Plas@Par.